Biology of Reproduction, 2022, **107(3)**, 800–812
https://doi.org/10.1093/biolre/ioac111
Advance access publication date 25 May 2022
Research Article

Bone morphogenetic protein 2- and estradiol-17β-induced changes in ovarian transcriptome during primordial follicle formation†

Prabuddha Chakraborty[1], Rebecca L. Anderson[2] and Shyamal K. Roy[2,3,*]

[1]Department of Genetics, University of North Carolina at Chapel Hill, Chapel Hill, NC, USA
[2]Department of Obstetrics and Gynecology, University of Nebraska Medical Center, Omaha, NE, USA
[3]Department of Cellular and Integrative Physiology, University of Nebraska Medical Center, Omaha, NE, USA

***Correspondence:** Departments of OB/GYN and Cellular and Integrative Physiology, 984515 Nebraska Medical Center, Omaha, NE 68198-4515, USA. Tel: +14025596163; E-mail: skroy@unmc.edu

†**Grant Support:** The study was supported by grants from NICHD (HD R01 HD093887), Olson Center for Women's Health (UNMC), Janssen Funds (UNMC) and Lagachulte and Weese Research funds (UNMC).

Abstract

Estradiol-17β has been shown to promote primordial follicle formation and to involve bone morphogenetic protein 2 (BMP2) as a downstream effector to promote primordial follicle in hamsters. However, the molecular mechanism whereby these factors regulate ovarian somatic cells to pre-granulosa cells transition leading to primordial follicle formation remains unclear. The objective of this study was to determine whether BMP2 and/or estradiol-17β would regulate the expression of specific ovarian transcriptome during pre-granulosa cells transition and primordial follicle formation in the mouse ovary. BMP2 mRNA level increased during the period of primordial follicle formation with the concurrent presence of BMP2 protein in ovarian somatic cells. Estradiol-17β but not BMP2 exposure led to increased expression of ovarian BMP2 messenger RNA (mRNA), and the effect of estradiol-17β could not be suppressed by 4-[6-[4-(1-Piperazinyl)phenyl]pyrazolo[1,5-a]pyrimidin-3-yl]quinoline dihydrochloride (LDN) 193189. BMP2 or estradiol-17β stimulated primordial follicle formation without inducing apoptosis. Ribonucleic acid-sequence analysis (RNA-seq) of ovaries exposed to exogenous BMP2 or estradiol-17β revealed differential expression of several thousand genes. Most of the differentially expressed genes, which were common between BMP2 or estradiol-17β treatment demonstrated concordant changes, suggesting that estradiol-17β and BMP2 affected the same set of genes during primordial follicle formation. Further, we have identified that estradiol-17β, in cooperation with BMP2, could affect the expression of three major transcription factors, GATA binding protein 2, GATA binding protein 4 and Early growth response 2, and one serine protease, hepsin, in pre-granulosa cells during primordial follicle formation. Taken together, results of this study suggest that estradiol-17β and BMP2 may regulate ovarian gene expression that promote somatic cells to pre-granulosa cells transition and primordial follicle formation in the mouse ovary.

Summary Sentence
BMP2 and estradiol-17β may regulate the transition of somatic cells to pre-granulosa cells, leading to the formation of primordial follicles in the murine ovary by upregulating key ovarian transcriptome.

Keywords: bone morphogenetic protein-2, estradiol 17β, primordial follicle formation, ovary, development

Introduction

Successful establishment of a primordial follicle (PF) pool is essential to maintain the supply of growing follicles throughout the reproductive life of mammals. In most mammals, PFs are formed in utero or shortly after birth [1] and its depletion coincides with reproductive senescence. In human, early depletion of the PF pool results in premature ovarian failure with consequent early onset of osteoporosis, cardiovascular, and cognitive disorders [2]. The PFs are characterized by an oocyte encircled by a layer of flattened granulosa cells. During embryonic development of the mouse ovary, somatic cells (SCs) adjacent the germ cell nests differentiate into flattened pre-granulosa cells (pre-GC), invade the nests, and surround individual oocytes to form PFs [1]. The process of PF assembly starts from E17.5 and continues until P3 in developing mouse ovaries with the appearance of morphologically distinct PFs on the first day of the postnatal life (P1).

The PF assembly in developing murine ovary is regulated by many factors, including growth factors, transcription factors (TFs), and hormones [3]. Several of the transforming growth factor beta family of proteins, including activin A, bone morphogenetic factor (BMP)-15, and growth and differentiation factor−9, have been shown to affect follicular development in mammalian ovaries [4–6]. The bone morphogenetic protein 4 (BMP4) induces primordial germ cell or oogonial apoptosis in vitro in 8–9-week-old human fetal ovary when oogonial proliferation occurs [7]; however, whether BMP4 affects oocyte viability is not known. We have not observed any effect of BMP4 on PF formation or oocyte apoptosis in E16 mouse ovaries or E15 hamster ovaries cultured for 4 or 8 days, respectively (unpublished observation). The bone morphogenetic protein 2 (BMP2) promotes PF assembly in developing hamster ovaries [8] and contributes to the development of primordial germ cells in the mouse [9]. The BMP2 is a secreted ligand that can regulate cell growth and differentiation in autocrine and paracrine fashion [10]. The BMP2 is known to facilitate the differentiation of osteoblasts, cardiomyocytes, and neuronal cells [11–13]. The BMP2 is also necessary for motility and the invasion of human trophoblast cells and several types of cancer cells [14–16]. In rodents and humans,

Received: January 3, 2022. **Revised:** March 22, 2022. **Accepted:** May 14, 2022

BMP2 expression has been observed in developing ovaries around the time of PF formation [7, 8, 17]. The BMP2 action is mediated by the heterodimer of activin receptor type 1 (ACVR1, Activin receptor like kinase 2 (ALK2), bone morphogenetic protein recetor 1A (BMPR1A, activin receptor like kinase 3, ALK3) or bone morphogenetic protein receptor 1B (BMPR1B, activin receptor like receptor kinase 6, ALK6), and BMPR2 [10]. Deletion of *Bmp2* in mice is embryo lethal [9]. Despite this information, the effect of BMP2 on oocyte or early follicular development in mice is not fully understood.

Among reproductive hormones, estradiol-17β (E2) promotes PF formation in hamsters and baboons [18–20]. In hamsters, facilitation of PF formation by exogenously added E2, both in vitro and in vivo, depends on E2 concentration. While lower concentrations support PF formation, higher concentrations are deleterious [18]. During development, fetal ovaries in utero are exposed to higher species specific levels of E2 [18, 21–23]. Higher levels of E2 are present in both maternal and fetal circulation from E16 through birth in mice [22]. Further, aromatase and 3β- hydroxysteroid dehydrogenase are expressed in the developing ovaries of humans, hamsters, and mice [18, 22, 24, 25]. Disruption of E2 action by an aromatase inhibitor, letrozole, results in reduced PF formation in baboons [20]. On the other hand, administration of high concentrations of E2 in vivo has been shown to inhibit germ cell nest breakdown during the postnatal development in mice [26, 27]. Therefore, the possible role of E2 on pre-GC transition leading to PF formation warrants further investigation.

The E2 is known to regulate BMP2 expression in several cell types, including osteogenic and mesenchymal cells in mice [28–30] and in hamster developing ovaries [31]. The E2 has been shown to modulate BMP2 promoter activity in mouse mesenchymal cells via canonical estrogen receptors, estrogen receptor 1 (ESR1) and estrogen receptor 2 (ESR2) [28]. Further, E2 seems to act via BMP2 as a upstream effector to promote PF formation in the hamster [31]. However, it is unclear if E2 and/or BMP2 affects the expression of specific ovarian genes during PF formation. Therefore, we sought to determine (1) if BMP2 or E2 would stimulate PF formation in the mouse ovary and (2) which ovarian genes would be affected by BMP2 or E2 during SCs to pre-GC cells transition, which was a prerequisite for PF formation.

Materials and methods

Animals and reagents

The CD1 mice were purchased from Charles River Laboratories, Wilmington, MA, USA, and were housed in a temperature- and humidity-controlled environment with 14-h light and 10-h dark cycles, and were fed ad libitum according to the UNMC Institutional Animal Care and Use Committee guidelines. The use of mice in this study was approved by the UNMC IACUC and NIH. Mice were time-mated, and fetal (E16 and E18) or postnatal (P1) ovaries free off extraneous tissue were collected in α-MEM with 0.5% BSA, 100 IU penicillin and 100 microgram streptomycin per ml (final). For in vivo studies, one set of ovaries were fresh frozen in optimal cutting temperature (OCT) compound for sectioning and immunofluorescence localization of BMP2, GATA2, GATA4, EGR2, and hepsin (*Hpn*), and the other set of ovaries were immediately placed in TRIZOL (Invitrogen, MA) for total RNA extraction [32, 33]. For in vitro studies, E16 ovaries were collected and cultured as described in respective experimental designs.

Sources for antibodies to BMP2, forkhead box L2 (FOXL2), GATA2, GATA4, EGR2, hepsin, and germ cell-specific nuclear antigen (GCNA) are presented in Supplementary Table 1. All antibodies were quality control-checked and their specificity was checked in the laboratory using positive control tissue sections and western immunoblotting. Primers for qPCR analysis are listed in Supplementary Table 2. Plastic embedding medium (Electron Microscopy Sciences, Hatfield, PA), Tissue-Tek optimum cutting temperature (OCT) compound (Sacura Finetek USA Inc., Torrance, CA), Phenol red-free α-MEM (GIBCO/Invitrogen, Waltham, MA), linolenic acid and BSA (Sigma Chemical Company, St. Louis, MO), LDN193,189 (Tocris, Minneapolis, MN), human holotransferrin, human insulin and selenium (BD Biosciences, San Jose, CA), RNA isolation kit (Qiagen, Germantown, MD), and Superscript reverse transcriptase and SsoAdvanced quantitative polymerase chain reaction (qPCR) kit (Bio-Rad, Hercules, CA) were purchased accordingly. The qPCR primers were synthesized by Thermo Fisher Scientific (Waltham, MA). All other molecular grade chemicals were purchased from various sources.

Effect of BMP2 or E2 on ovarian BMP2 mRNA expression and PF formation

Both BMP2 mRNA and protein expression were examined to determine whether BMP2 was expressed in vivo in the developing mouse ovary prior to morphologically distinct PF formation and also to determine whether either BMP2 or E2 would upregulate *BMP2* mRNA expression and promote PF formation in vitro. E16 ovaries were cultured with or without E2 or BMP2 for 4 days (C4) for in vitro experiment. It has been shown that oogonia start entering meiotic prophase by E13.5 to become oocytes and most of the oocytes enter the pachytene stage by E16 [34]. We have also observed that >95% oocytes complete entering the pachytene stage by E16 but morphologically distinct PFs are absent on E16 in CD1 mice. Therefore, the rationale for using E16 ovaries was that morphologically distinct PFs were absent and oogonia to oocyte transition was over; hence, any effect on PF formation would most likely reflect SCs to pre-GC transition. There were at least three ovaries from different fetuses for each in vivo day of development for localization experiment, whereas for each in vitro replicate, E16 ovaries were collected from many fetuses of different mothers in phenol red-free α-MEM containing penicillin, streptomycin, and 0.25 microgram per ml amphotericin B at room temperature, which were cleaned and cultured for 4 days (C0–C4) on tissue culture inserts placed in 1 ml phenol red-free α-MEM in presence of 0.1 μg/ml insulin, 1.25 μg/ml transferrin, 1.25 μg/ml selenium, and 10.7 μg/ml linoleic acid on culture inserts with 3-μm pores (Falcon, Fisher Scientific) as described for the hamster ovaries [18, 31]. The E2 (3.67 nM in 1 μl ethanol) and recombinant human BMP2 (R&D Systems, Inc., Minneapolis, MN, 50 ng in 2.5 μl 0.1% BSA/4 mM HCl) were added at the beginning (C0) of culture and every 48 h. The LDN 193,189 (0.5 μM final in 5 μl dimethyl formamide), an ACVR1 and BMPR1A inhibitor, was added at C0 with or without BMP2 or E2. No deleterious effect was noted for the volume of ethanol or DMF used in culture (data not shown). Ovaries were retrieved for morphometric analysis, immunofluorescence detection of antigens or RNA preparation for RT-qPCR analysis. For morphometric analysis of PFs, ovaries were fixed in Bouin's fixative for 24 h, dehydrated by grades of ethanol, cleared with JB4 plastic resin, and embedded in JB4 plastic as suggested by

the manufacturer (EM Sciences, Hatfield, PA). Blocks were cut at 5-mm thickness, stained with Harris's hematoxylin, dehydrated by ethanol grades, and mounted with Dibutylphthalate Polystyrene Xylene (Millipore-Sigma, St. Louis, MO). We counted every fifth section to obtain raw number of oocytes and PF in selected sections of each ovary for each group. The total numbers of oocytes and PFs present in the whole ovary were estimated by multiplying the raw counts by five to correct for uncounted sections using the method described by Sarma et al. [35]. Minimum three ovaries from different animals were used per group to calculate the mean ± standard error of mean (SEM). Cytotoxic effect of BMP2 or E2 doses were also examined by cleaved caspase 3 immunofluorescence localization.

RNA sequencing

To determine the effect of BMP2 and E2 on transcriptome of developing ovaries before the appearance of morphologically distinct PF, E16 ovaries were exposed to either vehicle, recombinant BMP2 (50 ng/μl), or E2 (3.67 nM) in vitro for 24 h. There were three replicates from different animals for each group. Total RNA was isolated using a Qiagen microkit and the quality of RNA was checked by a RNanalyzer (UNMC DNA Core). The RNA samples with RIN value >9 were used for making sequencing libraries with Illumina True-Seq RNA Sample Preparation V2 kit (UNMC DNA Core Facility). Libraries were sequenced using Illumina NextSeq500, yielding 75-bp single end reads in the UNMC DNA Core facility.

Reads were trimmed as necessary by Trim Galore (https://www.bioinformatics.babraham.ac.uk/projects/trim_galore/) followed by alignment using Tophat2 [36]. The aligned reads were counted by HTseqCount [37] and differential expression analysis was done by DESeq2 [38] using recommended parameters. The gene ontology (GO) pathway enrichment analysis was performed by ClusterProfiler [39] and Gene Set Enrichment Analysis (GSEA; 4.1.0) [40]. Subsetting and other data wrangling was performed in "R" (3.6.2) and with dplyr (0.8.3), data plots were made by using ggplot2 (3.2.1), ggpubr (0.2.4) and enhancedVolcano (1.4.0).

Isolation of ovarian RNA and RT-qPCR analysis of selected transcripts

First, we short listed BMP2 or E2-responsive genes based on their likelihood of affecting ovarian cell functions. From the list, we selected *Gata2*, *Gata4*, and *Egr2* based on (1) their reported role in ovarian follicular development and (2) the availability of validated and authenticated antibodies for further examination. This was particularly true for *Tmprss11a* gene, which was a serine protease-coding gene (Figure 3A), a HAT/DESC subfamily member of type II transmembrane serine proteases (TTSP) [41, 42]. Although members of TTSP family of proteases had been shown to play an important role in cell adhesion or migration [43], we could not assess *Tmprss11a* beyond mRNA expression because of the unavailability of specific and valid reagents. Serendipitously, we identified hepsin, a member of the hepsin/transmembrane serine protease (hepsin/TMPRSS) subfamily [41] of TTSP, for which validated antibody was available. Therefore, we decided to examine the expression of *Hpn* along with three selected TFs. Ten nanograms of total RNA were reverse-transcribed in a 20-μl reaction mixture using the superscript RT kit (Bio-Rad) as suggested by the manufacturer, and 1 μl cDNA mix was amplified for 40 cycles using SYBR green qPCR kit and gene-specific primer sets in a Bio-Rad thermocycler. Glyceraldehyde-3-phosphate dehydrogenase (*Gapdh*) gene was used as a housekeeping gene to normalize the qPCR data across treatment groups. The qPCR primer sequences are presented in Supplementary Table 2. The *Gapdh* was selected after testing several commonly used housekeeping genes based on its stable expression regardless of the treatment condition. Gene-specific Ct values were calculated based on the manufacturer's formula, normalized against corresponding *Gapdh* values, and mRNA levels relative to E16 (in vivo) or control culture (in vitro) were calculated for each replicate. Then values of at least three replicates from different animals were used to derive the mean + SEM.

Immunofluorescence localization of BMP2, FOXL2, GATA2, GATA4, EGR2, hepsin, GCNA, or cleaved caspase 3

In vivo-developed ovaries were cleaned of extraneous tissue in 30% sucrose-/phosphate-buffered saline, pH 7.4, and frozen in OCT. In vitro-cultured ovaries were placed in 30% sucrose/PBS on ice for 10 min and were then frozen in OCT. Fresh frozen sections (6 μM) were fixed in 4% freshly made paraformaldehyde at 10°C as described previously [18, 31, 44]. Sections were incubated overnight at 4°C with antigen-specific antibodies and were probed with host-specific second antibody conjugated to different Alexa dyes. Nuclei were stained with DAPI. To determine the specificity of in vivo BMP2 immunosignal, sections of E18 ovaries were incubated with BMP2 antibody preneutralized with 200 ng of recombinant human BMP2. Sections were examined and were imaged in a Leica confocal microscope and were then overlayed to depict the cell-type specific expression. Because the confocal microscope could detect only RGB and one far-red fluorophore, the DAPI signal (blue of RGB) was assigned gray pseudocolor to identify follicle structure and cells in ovary sections.

Immunosignal was semi-quantitated using Image J (NIH) density quantification module. For each overlayed image, there were four image planes showing individual fluorescence signal. Many image sets were captured to cover the entire ovary section. Because we wanted to know cell types expressing a particular gene signal and whether the expression was influenced by BMP2 or E2, we used FOXL2 as a marker for pre-GC because FOXL2 was considered as a verified marker for granulosa cells and as authenticated antibody against FOXL2 was commercially available. First, the intensity of fluorescence for a particular protein in individual somatic cells (SCs) in an image was measured. Then, we identified FOXL2-positive (pre-GC) or FOXL2-negative (non-GC) cells. Next, we calculated the average of cell-type specific fluorescence intensity for the entire section representing one ovary. We repeated the same for sections from other ovaries of individual experimental groups, and then, the average values for three or more ovaries of individual groups were used for calculating the mean for each experimental group. Cell-type specific means of either in vivo or in vitro experimental groups were analyzed for statistical significance and to derive the standard errors of mean. To keep the analysis focused on SCs, no attempt was made to include oocytes in the analysis.

Statistical analysis

All quantitative data were analyzed by one-way ANOVA or "*t*" test as needed with Tukey's correction. The values were considered to be of significance if the *P* values were <0.05.

Although many data had P values < 0.01 or less, $P < 0.05$ was used throughout to indicate significance for consistency.

Results

Expression of BMP2 in developing ovaries in vivo, and the effect of BMP2 or E2 on BMP2 mRNA expression and PF formation in vitro

The *BMP2* mRNA levels increased sharply by E18 and remained stable through P1(Figure 1A). The E2 but not BMP2 significantly ($P < 0.05$) stimulated *BMP2* mRNA expression in E16 mouse ovaries after 4 days of culture (C4, equal to P1, Figure 1B). The LDN193,189, an ACVR1and BMPR1A blocker failed to inhibit E2-induced increase in *BMP2* mRNA, thus ruling out the possibility of a BMP2 autoregulatory effect (Figure 1B). Robust BMP2 immunosignal (green) in the cytoplasm of oocytes (red) and FOXL2-positive pre-GC (blue) was evident in E18 ovaries (Figure 1C). Surface epithelial cells (arrowheads) and FOXL2-negative cells (arrows) were mostly BMP2-negative (Figure 1C). The BMP2 immunosignal was almost undetectable in sections incubated with preneutralized antibody (Figure 1D). The BMP2 or E2 significantly ($P < 0.05$) upregulated the total number of PFs in the ovary without affecting the total number of oocytes (Figure 1E). No apparent difference in cleaved caspase 3 localization in oocytes or SCs was evident in vehicle- (Supplementary Figure S1A), BMP2- (Supplementary Figure S1B), or E2-exposed ovaries (Supplementary Figure S1C), indicating that the dose of BMP2 or E2 was unlikely to adversely affect the ovarian cells, although no quantitation was attempted.

Effect of BMP2 and/or E2 on ovarian transcriptome around the time of PF formation

The BMP2 treatment in the E16 ovaries for 24 h upregulated 597 genes and downregulated 585 genes (Figure 2A) (P-adjust < 0.05). The GO biological pathway enrichment analysis of differentially expressed genes (DEGs) predictively revealed enrichment of cellular processes associated with reproduction such as meiotic cell cycle and female gamete generation (Figure 2B). Additionally, epithelial cell proliferation, angiogenesis, and cellular pathways involving apoptosis signaling and ribonucleoprotein biogenesis were significantly altered due to BMP2 treatment (Figure 2B). To predict the downstream effector pathways affected by the upregulated and downregulated gene sets due to BMP2 exposure, these gene sets were compared to the GO molecular functions. Enrichment of pathways associated to protein translation in >1.5-fold downregulated genes and inhibitor of endopeptidase activity in the rest of the downregulated genes indicated potential inhibition of protein anabolism (Figure 2C). On the other hand, activities of increased serine peptidase, serine endopeptidase, and serine hydrolase showed enrichment in the 1.5-fold upregulated genes, suggesting possible matrix remodeling (Figure 2C). Analysis of the DEGs with GSEA further revealed significant (FDR < 0.01) enrichment of DNA-binding transcription activity (Figure 2D). The constituent TF genes in this pathway were mostly upregulated by BMP2, and the list included *Folliculogenesis Specific BHLH transcription factor (Figla)*, *LIM homeobox 8 (Lhx8)*, *NOBOX oogenesis homeobox (Nobox)*, and *Spermatogenesis And Oogenesis Specific Basic Helix-Loop-Helix 1 (sohlh1)* (Figure 2E). Further, BMP2 also upregulated several granulosa cell-specific TFs, such as *Foxl2*, *Gata4*, and *Egr2* (Figure 2E).

The E2 treatment for 24 h in E16 ovariesupregulated1852 genes and downregulated 1780 genes (P-adjust < 0.05) (Figure 3A). The GO biological pathway enrichment analysis on these DEGs revealed enrichment of reproductive and urogenital system development, epithelial cell proliferation and cell migration, and Wnt signaling pathway (Figure 3B). Further, among GO molecular functions, pathways related to ribosomes and cytoskeleton were enriched in the downregulated genes (Figure 3C). Moderately upregulated genes (<1.5-fold) affected the ATPase and helicase activities in addition to the pathways related to mRNA and ribonucleoprotein binding. Pathways involving channel and transporter activities were enriched in the upregulated genes >1.5-fold (Figure 3C). Further, E2 also significantly upregulated oocyte-specific TFs, such as *Figla*, *Lhx8*, *Nobox*, and *Sohlh1* (Figure 3D). Significant upregulation of *Gata2* (expressed mostly in primordial oocytes) [45] and *Gata4* (expressed in granulosa cells) [46] also occurred by E2. When the effect of BMP2 was compared with E2, 87% of 721 common DEGs were either upregulated (272 genes) or downregulated (353 genes) concordantly (Figure 4A). Further, pathway enrichment analysis with these common DEGs suggested enrichment of genes involved in DNA modification during gamete formation and insulin-like growth factor response pathways (Figure 4B). On the other hand, pathways pertaining to ribosome, mRNA-binding, and translation activity were enriched in downregulated genes (Figure 4C).

To further determine how changes in gene expression in response to either BMP2 or E2 affects granulosa cell differentiation, DEGs ($P < 0.05$) from either BMP2- or E2-treated samples were compared with the gene signatures from differentiating bipotential granulosa cells (D-BPGs) and differentiating epithelial granulosa cells (D-EPGs) during the same developmental timeframe before PF formation [47]. Clustering among the common genes between DEGs and D-BPG signature or D-EPG signature genes revealed four or five major clusters (Supplementary Table 3), respectively (Figure 4D and E). Among D-BPG signature genes, BMP2 exposure led to upregulation in clusters 3 and 4 (CL3 and CL4) and minimal downregulation of a small subset in CL2 (Figure 4D). On the other hand, E2 exposure led to upregulation of the CL1 and CL4 and downregulation of CL2 and CL3 (Figure 4D). Among D-EPG signature genes, BMP2 exposure downregulated part of CL1 and CL4 and upregulated CL2 (Figure 4E). The E2 treatment led to downregulation of most of the genes represented in CL4 and CL5, while showing upregulation in CL1 and CL3 (Figure 4E). Overall, BMP2 treatment led to upregulation of majority of D-BPG signature genes, whereas D-EPG signature remained relatively unaffected by BMP2, while E2 showed small but distinct upregulation of a part of D-BPG and D-EPG and downregulation of other D-EPG signature.

Expression of *Gata2*, *Gata4*, *Egr2* and *HPN* mRNA, and proteins in ovarian SCs in vivo

The *Gata2*, *Gata4*, *Egr2* and *HPN* mRNA were not only expressed in E16 ovary (Figure 5A–D), but their levels increased significantly ($P < 0.01$) by E18 and P1 (Figure 5A, B, and D).

The intensity of GATA2 immunosignal was significantly higher ($P < 0.05$) in pre-GC compared to non-GC throughout

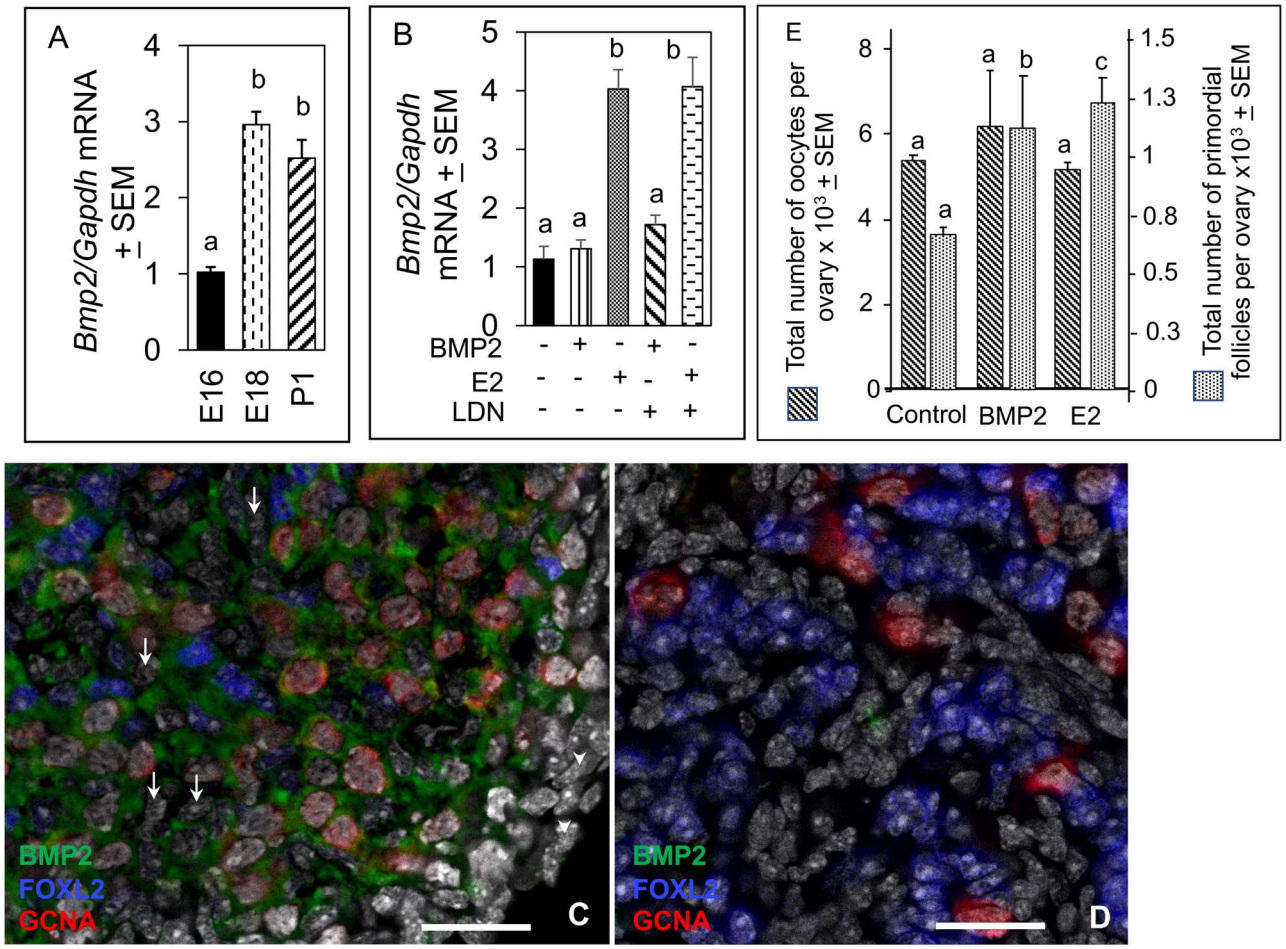

Figure 1. BMP2 expression in the developing mouse ovary and effect of BMP2 or E2 on PF formation in vitro. (A) qPCR quantitation of *BMP2* mRNA expression in vivo in E16, E18, and P1 ovaries. Each bar represents the ratio of *BMP2* and *GAPDH* ± SEM. (B) qPCR quantitation of *BMP2* mRNA expression in vitro in either vehicle (0.1% ethanol), BMP2- or E2-exposed ovaries in the presence or absence of 500 μM BMPR inhibitor, LDN193,189. Each bar represents the ratio of *BMP2* and *GAPDH* ± SEM. Bar = 25 μm. Bars with same letter, P > 0.05; bars with different letter, P < 0.05. (C-D) Localization of BMP2 in 18-day old fetal mouse ovary incubated overnight with a BMP2 antibody (C) or BMP2 antibody neutralized with 200 ng recombinant human BMP2 (D). BMP2 (green), FOXL2 (blue), GCNA (red), and DAPI (gray). PF formation in response to either BMP2 or E2 in vitro (E). Number of oocytes in the control group was compared with those of BMP2- or E2-treated group. Similarly, number of PFs in the control group was compared with those of BMP2- or E2-treated group. Bars with different letter within each cell type category, $P < 0.05$; bars with same letter within each cell type category, $P > 0.05$.

development, with clear presence of the protein in the cell nuclei (Figure 6A, insets, Supplementary Figure S2). The intensity of GATA2 signal in pre-GCs increased ($P < 0.01$) further on E18 (Figure 6A–D). Distinct GATA2 immunofluorescence was evident in FOXL2-positive pre-GCs as well as in non-GCs of E18 ovaries (Supplementary Figure S3). While modest GATA2 immunosignal was present in the oocytes of E16 and E18 ovaries (Figure 6A and B), marked increase was evident by P1 (Figure 6C). The intensity of GATA4 immunosignal was significantly more ($P < 0.05$) in pre-GCs compared to non-GCs on E16 (Figure 6E and H), although not all pre-GCs were GATA4-positive. The GATA4 signal intensity increased significantly by E18 through P1 (Figure 6F–H). Remarkable variation in FOXL2 immunofluorescence across pre-GCs affected the image of GATA4 fluorescence by often masking the gene-specific signal (Figure 6F and G). Higher magnification images of individual image planes clarified the statement (Supplementary Figure S4). Nuclear localization of EGR2 protein was visible in pre-GC (Figure 6I–L, arrows). The EGR2 immunostaining was absent in non-GC (arrowheads, Figure 6J and K). Distinct cytoplasmic immunosignal was evident in the oocytes on P1 (Figure 6K, broken circles). Higher magnification images of primordial or primary follicles on P1 depicted strong nuclear EGR2 staining in some of the surrounding granulosa cells (Figure 6K, insets, arrows). Signal intensity increased significantly ($P < 0.05$) in pre-GC by E18 before declining by P1 (Figure 6L).

Diffused cytoplasmic and matrix localization of hepsin was evident, primarily around non-GC in E16 ovary sections (Figure 6M). However, *Hpn* immunosignal gradually localized around pre-GC on E18 (Figure 6N, inset) and became prominent on P1 (Figure 6O). By P1, distinct cytoplasmic staining was noted in the oocytes and between pre-GCs of forming PFs (Figure 6O, inset, arrowhead).

Effects of BMP2 or E2 on the expression of *Gata2*, *Gata4*, *Egr2* and mRNA and proteins in ovarian SCs in vitro

The BMP2 or E2 significantly ($P < 0.01$) augmented the levels of *Gata2*, *Gata4*, *Egr2*, and *HPN* mRNA in 4 days (C4) cultured ovaries, although the effect of E2 on *Gata4* and

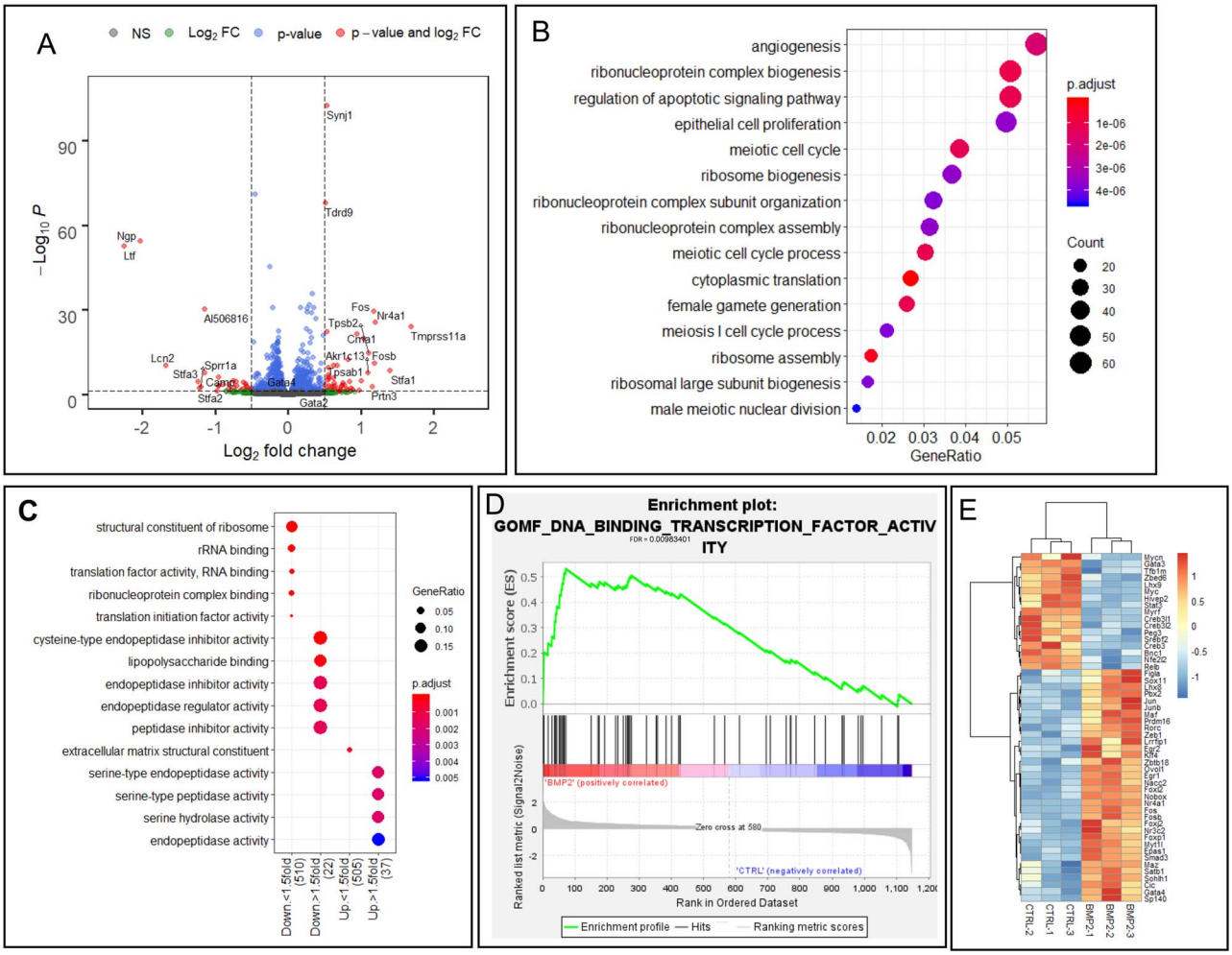

Figure 2. BMP2 regulation of ovarian gene expression during development. (A) Volcano plot showing changes in gene expression in all genes upon BMP2 exposure in developing ovary in vitro. Gray dots, $P > 0.05$ and FC < 1.5-fold; green dots, $P > 0.05$, FC > 1.5-fold; blue dots, $P < 0.05$, FC < 1.5-fold; red dots, $P < 0.05$, FC > 1.5-fold. Vertical dotted lines show 1.5-fold cutoff and horizontal dotted line shows $P = 0.05$ cutoff. (B) GO biological pathway enrichment analysis with all differentially expressed genes (DEGs) ($P < 0.05$) upon BMP2 treatment compared to untreated control. (C) GO molecular function pathway enrichment analysis with same geneset. (D) GSEA with all DEGs upon BMP2 exposure compared to untreated control. (E) Heatmap showing all the TFs from the geneset in (D) prepared with normalized counts from untreated and BMP2-treated samples with row-centered color scheme.

Egr2 mRNA levels was significantly less than that of BMP2 (Figure 7A–D). Effects of BMP2 or E2 on mRNA levels were completely suppressed by LDN193,189 suggesting that the effect of E2 was most likely mediated by BMP2 and the effect of BMP2 was specific (Figure 7A–D).

The GATA2 immunosignal was barely visible in pre-GC and was virtually nondetectable in non-GC SCs in ovaries cultured with vehicle only (control, Figure 8A). No signal was present in the oocytes (Figure 8A). The BMP2 exposure significantly increased GATA2 signal intensity in pre-GC (Figure 8B and D), especially those in the follicles. Whereas many oocytes showed remarkable increase in GATA2 intensity, some had no expression (Figure 8B). The E2 exposure further augmented GATA2 immunofluorescence signal in pre-GC (Figure 8C and D), especially of PFs (Figure 8C, broken circles), but noticeable increase also occurred in non-GC SCs (Figure 8D). The LDN193,189 virtually eliminated BMP2 or E2 effect on GATA2 immunosignal in all cells, including the oocytes (Supplementary Figure S5A and B). Most notably, LDN193,189 reduced FOXL2 immunosignal to such an extent that valid cell-type specific quantification was not possible. In the control group, a cohort of FOXL2-positive pre-GC showed detectable but variable GATA4 immunosignal, whereas non-GC SCs were barely positive (Figure 8E). The BMP2 significantly ($P < 0.01$) elevated GATA4 signal intensity in pre-GC, especially those in the follicles (Figure 8H and F, broken circles) and also in non-GCs. However, not all pre-GC in follicles or elsewhere in BMP2-exposed ovaries were positive or had similar signal intensity (Figure 8F). The E2 also elevated the intensity of GATA4 immunofluorescence signal, primarily in the pre-GC (Figure 8H). Higher magnification of individual image planes of an E2-exposed C4 ovary clearly depicted that strong FOXL2 immunofluorescence masked robust GATA4 immunosignal in FOXL2-positive cells (Supplementary Figure S6). Although not quantified, exposure to BMP2 or E2 seemed to increase the number of FOXL2-positive cells in cultured ovaries (Figure 8F and 8G). The LDN193,189 also suppressed GATA4 and FOXL2 fluorescence (data not shown). The EGR2 immunosignal was very low in the nuclei of pre-GC or non-GC in vehicle-exposed ovaries, but strong cytoplasmic staining was noted

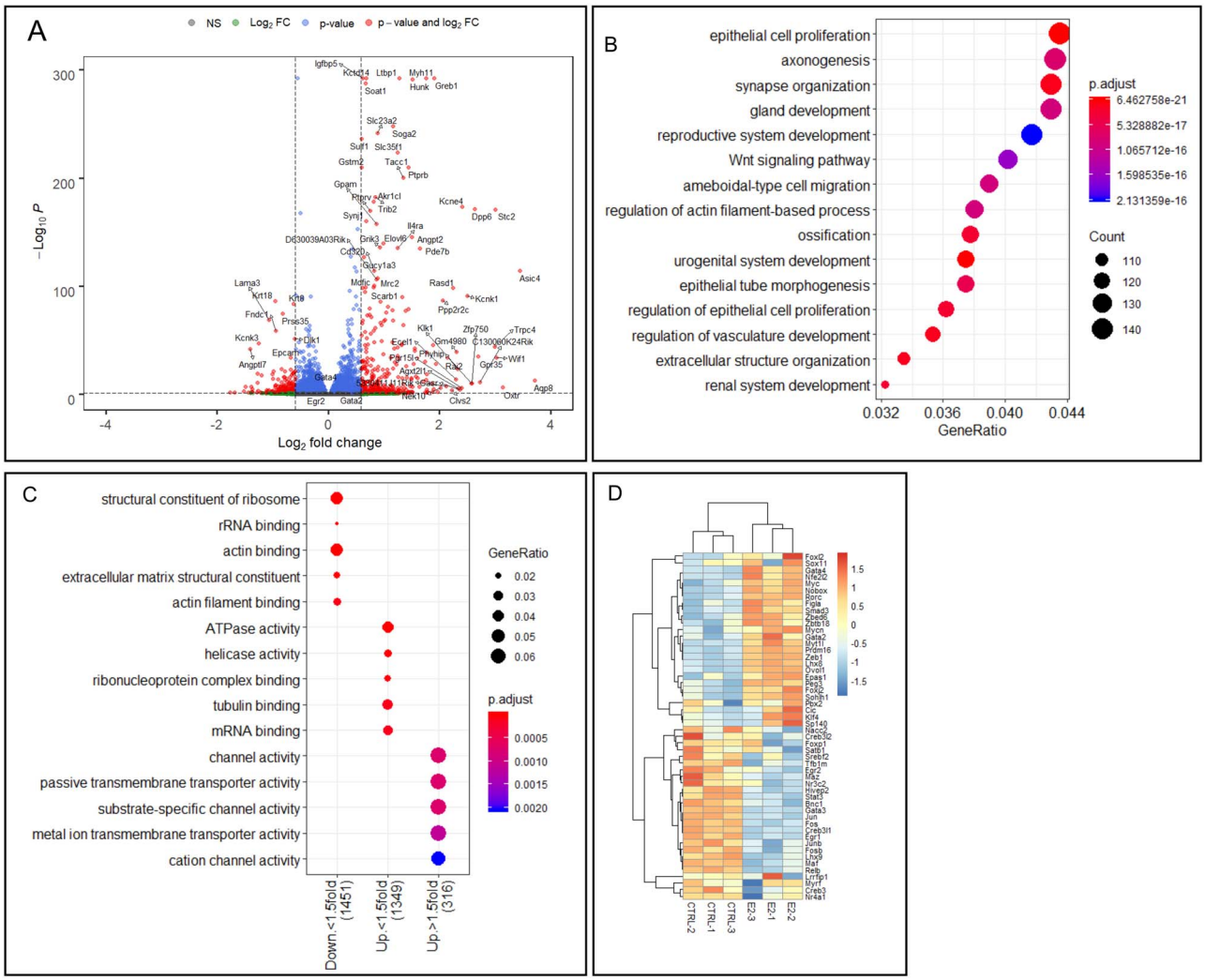

Figure 3. E2 regulation of ovarian gene expression during development. (A) Volcano plot showing changes in gene expression in all genes upon E2 exposure in developing ovary in vitro. Gray dots, $P > 0.05$, and FC < 1.5-fold; green dots, $P > 0.05$, FC > 1.5-fold; blue dots, $P < 0.05$, FC < 1.5-fold; red dots, $P < 0.05$, FC > 1.5-fold. Vertical dotted lines show 1.5-fold cutoff and horizontal dotted line shows $P = 0.05$ cutoff. (B) GO biological pathway enrichment analysis with all DEGs ($P < 0.05$) upon E2 treatment compared to untreated control. (C) GO molecular function pathway enrichment analysis with same geneset. (D) Heatmap showing all the TFs from the geneset in (D) prepared with normalized counts from untreated and E2-treated samples with row-centered color scheme.

for the oocytes (Figure 8I). The BMP2 or E2 significantly ($P < 0.01$) upregulated the EGR2 signal intensity primarily in the pre-GC clusters and the cells in the PF (Figure 8J–L, broken circle). Slight increase occurred in non-GC SCs. Modest hepsin immunosignal was present around pre-GC and oocytes in the control group (Figure 8M). The BMP2 or E2 elevated hepsin signal primarily around pre-GC clusters (arrowheads, Figure 8N and O). Because of ovarian matrix-based localization of hepsin immunosignal, no attempt was made to quantify the immunosignal.

Discussion

Transition of non-differentiated ovarian SCs into pre-GC cells is a prerequisite for the formation of PFs. Therefore, the correlation of BMP2 expression in the mouse ovary in vivo, induction of *BMP2* mRNA by E2 in vitro, and stimulation of PF formation in vitro by BMP2 tend to suggest that BMP2 may facilitate the transition of ovarian SCs into pre-GC in the mouse ovary similar to that observed for the hamster ovary [18, 31]. Human fetal ovary also expresses *BMP2* mRNA and protein by 8–9 weeks and the expression increases markedly by 14–16 weeks of fetal life [7]. The BMP2 promotes cell differentiation in human [48] and hamster fetal ovaries [31]. Upregulation of PF formation in the mouse ovaries by E2 corroborates our findings in the hamster [18, 31]. Appreciable levels of maternal or fetal E2 in E18.5 mice [22], increase in BMP2 in E18 mouse ovaries, and upregulation of BMP2 by E2 in vitro suggest that E2 may control BMP2 expression in the mouse ovary as well.

The E2 promotes in vivo PF formation in the hamster [18] and baboon [20]. The E2 levels in maternal and fetal plasma on E17.5- E18.5 [22] correspond to the time of pre-GC transition in vivo. However, 10^{-7} M (27.27 ng/ml) E2 in vitro has been shown to inhibit oocyte nest breakdown in mice, whereas lower concentrations have no effect [26, 49]. By contrast, 3.67 nM (1 ng/ml) E2 significantly promotes in vitro PF formation in fetal hamster ovaries [18] and in fetal mouse ovaries (present study) without affecting the total number of oocytes. However, increasing the dose to as small as 5 ng/ml severely increases cellular apoptosis and PF formation [18].

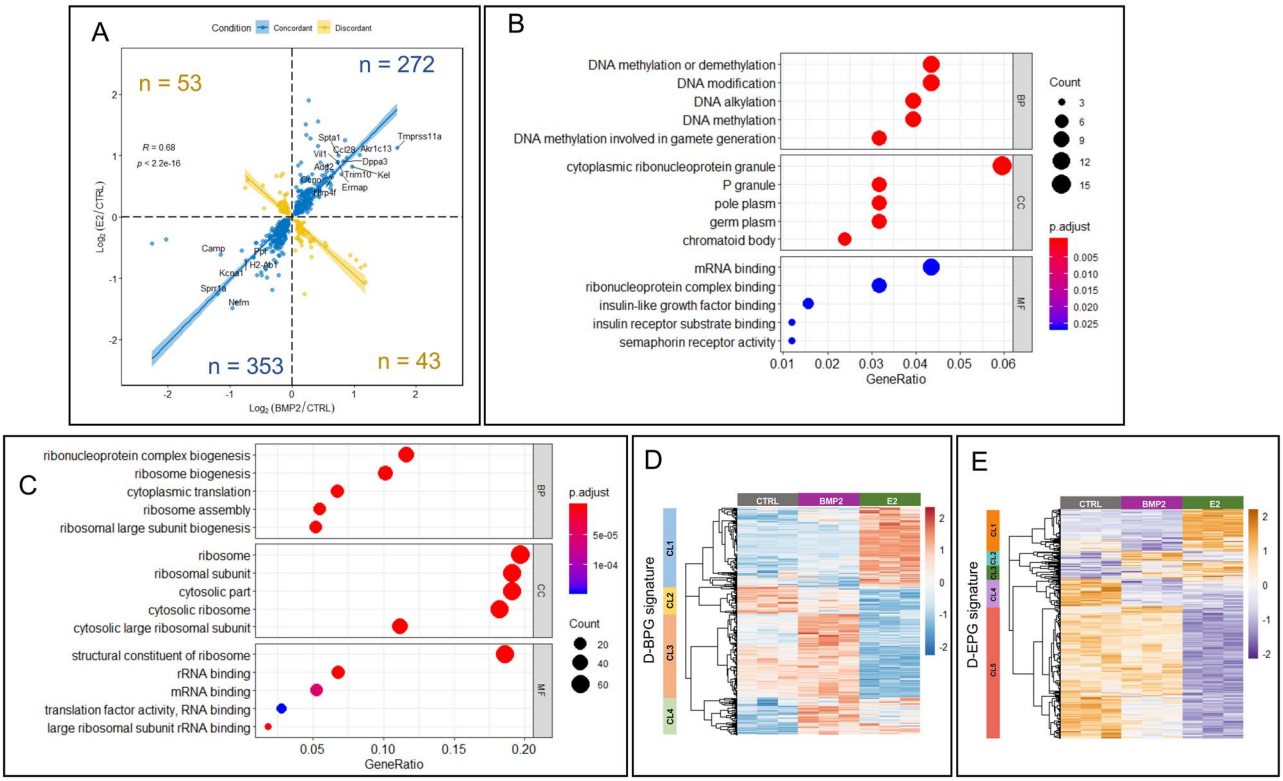

Figure 4. Regulation of gene expression in developing ovary by both E2 and BMP2. (A) Concordant (blue dots and line) and discordant (yellow dots and line) gene expression from either BMP2 treated versus untreated control ($P < 0.05$) or E2-treated versus untreated control ($P < 0.05$). Number of genes are represented in each quadrant. Spearman correlation coefficient $R = 0.68$, $P < 2.2e\text{-}16$. (B and C) GO pathway enrichment analysis from biological process ontology (BP), cellular component ontology (CC), and molecular function ontology (MF) with both concordantly upregulated (B) and concordantly downregulated (C) DEGs in response to either BMP2 or E2 treatment versus untreated control. (D and E) Clustered heatmap illustrating expression of DEGs from either BMP2- or E2-treated ovaries that overlapped with the gene signature for differentiating bipotential pre-GC cells (D-BPGs) (D) or differentiating epithelial pre-GC cells (D-EPGs) (E). Identified major clusters (CL) are represented in the left color-coded bar. Heatmap was prepared with normalized counts from either untreated or BMP2-treated or E2-treated samples with row-centered color scheme.

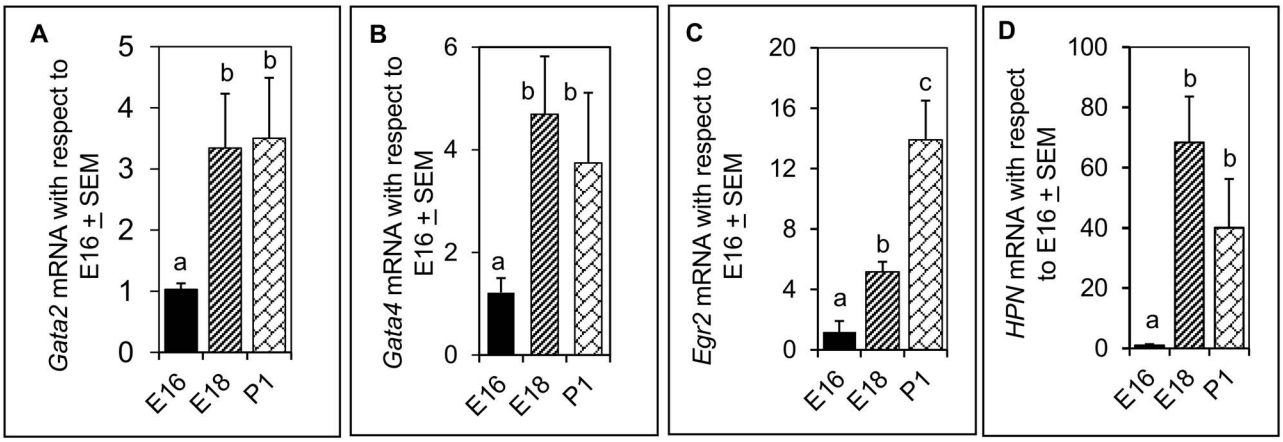

Figure 5. Fold changes in (A) *Gata2*, (B) *Gata4*, (C) *Egr2*, and (D) *HPN* mRNA relative to E16 levels during in vivo PF formation in the ovary. ΔCt values for each sample for each transcript were calculated using corresponding *GAPDH* Ct values to obtain ΔΔCt. Then 2^-(ΔΔct) value (fold change relative to E16 ovaries) for each sample was calculated based on the formula provided by the manufacturer (BIO-RAD) and was used to calculate the mean + SEMs. E16 and E18 represent fetal ages, and P1 represents postnatal day 1. Bars with same letter, $P > 0.05$; bars with different letters, $P < 0.05$.

Therefore, it is logical to assume that E2 upregulation of PF formation depends critically on the dose of E2. Deletion of ESR2 with or without ESR1 compromises fertility in mice, although PF formation occurs [50, 51]. However, deletion of classic ESR does not completely eliminate other avenues of E2 action. We have shown that *Gper1*, a membrane estrogen receptor, is expressed in hamster ovarian cells [52] and GPER1 can mediate E2 effect on ovarian PF formation [19, 32]. Further, an interactive regulatory role of GPER1 and FSHR in follicular function has been reported [53]. Whereas we do not know what compensatory mechanism in ESR knockout mice promotes PF formation, the results of the present study present a strong argument in favor of a facilitatory role of E2 perhaps via BMP2 on PF formation.

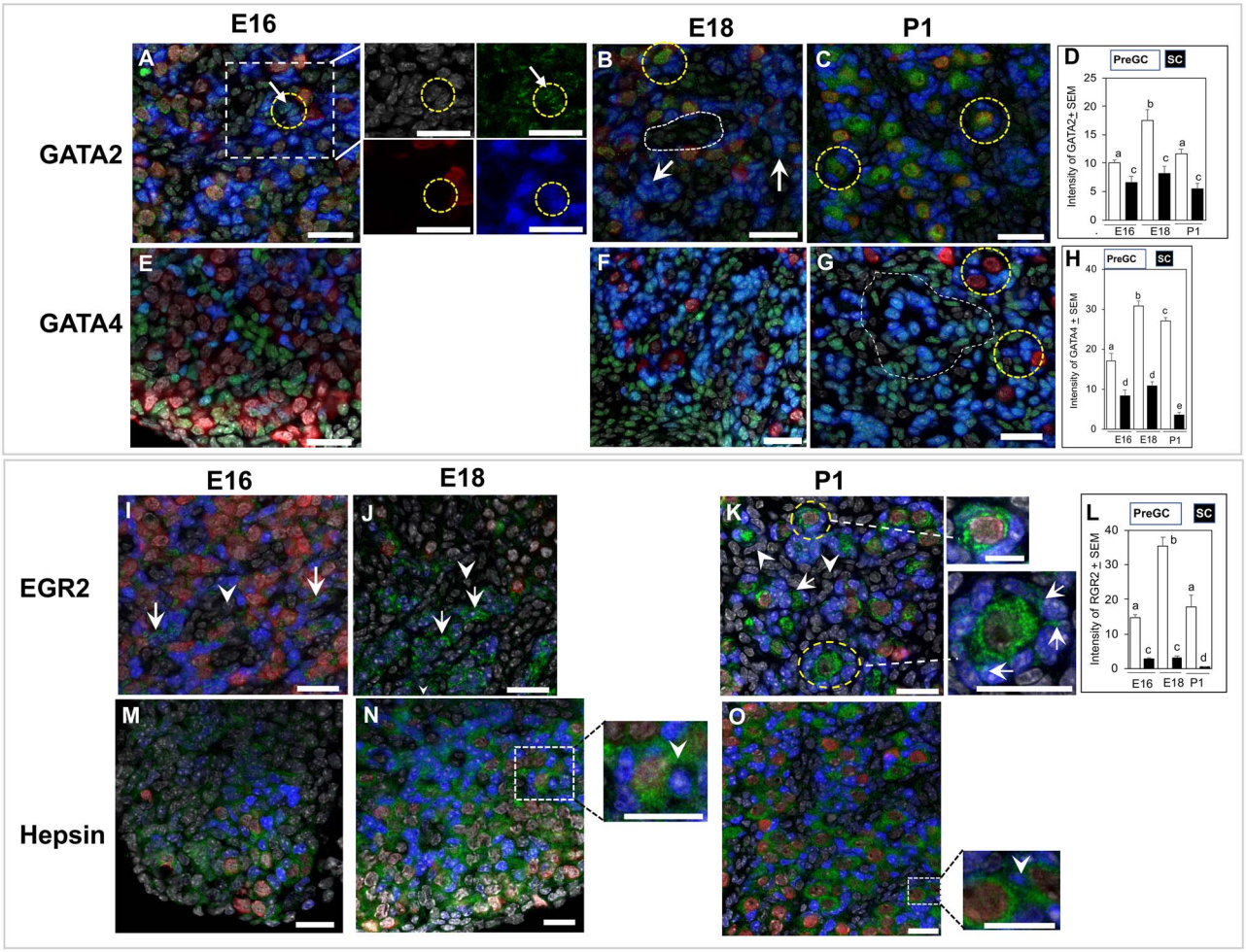

Figure 6. GATA2, GATA4, EGR2, and hepsin localization in sections of E16, E18, and P1 ovaries. (A–D) Nuclear localization (circle) of GATA2 (green) protein in E16 (A), E18 (B), and P1 (C) ovaries and quantitation of its immunosignal intensity (D). Arrows show FOXL2-positive pre-GC in E16 ovary (A). Arrows showing GATA2 signal in FOXL2-positive pre-GC in an E18 ovary (B). Broken circles indicate GATA2 staining in the oocytes on E18 (B) and P1 (C) ovaries. Broken line encircles a pool of non-GC cells (B). High intensity of FOXL2 (blue) often masked green fluorescence of GATA2. (E–H) GATA4 (green) localization in E16 (E), E18 (F), and P1 (G) and quantitation of its immunosignal intensity (H). Intense ovarian GATA4 immunosignal was present in pre-GC of E18 (F) and P1 (G) ovaries. Broken circles (G) showed pre-GC associated with PFs. Higher intensity of FOXL2 immunosignal masked GATA4 immunosignal forming teal-colored nuclei and presented an apparent higher expression in non-GC (area encircled by dotted line; see Supplemental Figures S3 and S4 for clarification). However, the difference in GATA4 immunosignal between two cell types was prominent in the bar graph (H). (J–M) EGR2 localization in E16 (J), E18 (K), and P1 (L) ovaries and quantitation of its immunosignal intensity (L). Nuclear localization of EGR2 protein (green) in FOXL2-positive pre-GC (arrows) and non-GC (arrowheads) in the E16 mouse ovary (I). EGR2 immunosignal in pre-GC on E18 (J) and P1 (K) ovaries (arrows). Cytoplasmic immunosignal in P1 ovary (inset). Higher magnification images of primordial or primary follicles in the P1 ovary (K) (insets). (M-O) Hepsin (green) localization in sections of E16 (M), E18 (N), and P1 (O) ovaries. Inset showing higher magnification image of hepsin staining between adjacent pre-GC in E18 and P1 ovaries (inset, arrowhead). Bars with same letter, $P > 0.05$; bars with different letters, $P < 0.05$. Green, target proteins; blue, FOXL2; red, GCNA; gray, nuclei. Bar = 25 μm.

Niu and Spradling [54] has shown that mouse pre-GCs develop from a ovarian surface epithelial-derived bipotential pre-GC cell (B-PGC) and a surface-epithelial derived epithelial pre-GC cell (E-PGC) lineages as early as E12.5. While B-PGC show robust FOXL2 expression by E12.5, E-PGC show it after birth [54]. Using the published gene signatures for D-BPGs and D-EPGs, which are similar to B-PGC and E-PGC based on characteristic gene expression [47, 54], the results of the present study demonstrate that among DEGs, BMP2 or E2 independently upregulates genes, which are potentially important for pre-GC transition. In the present study, characteristic expression of selected TFs in FOXL2-positive (pre-GC) and FOXL2-negative SCs suggests that these TFs may play a role in the differentiation of B-PGC or E-PGC lineages. It is tempting to postulate that BMP2 or E2 induction of selected TFs in FOXL2-positive pre-GC suggests a possible mechanism whereby these TFs affect FOXL2 expression and pre-GC transition. Alternatively, FOXL2 expression may be a consequence of pre-GC transition, which is induced by these TFs. Low-level expression of TFs in FOXL2-negative SCs may be adequate to regulate routine cell functions but inadequate to induce pre-GC transition. However, specific studies are needed to verify this conjecture.

Increased expression of GATA2 in vivo with developmental age and upregulation by BMP2 or E2 suggests that this TF may regulate at least some aspects of PF formation. Siggers and coworkers [55] have documented that ovarian expression

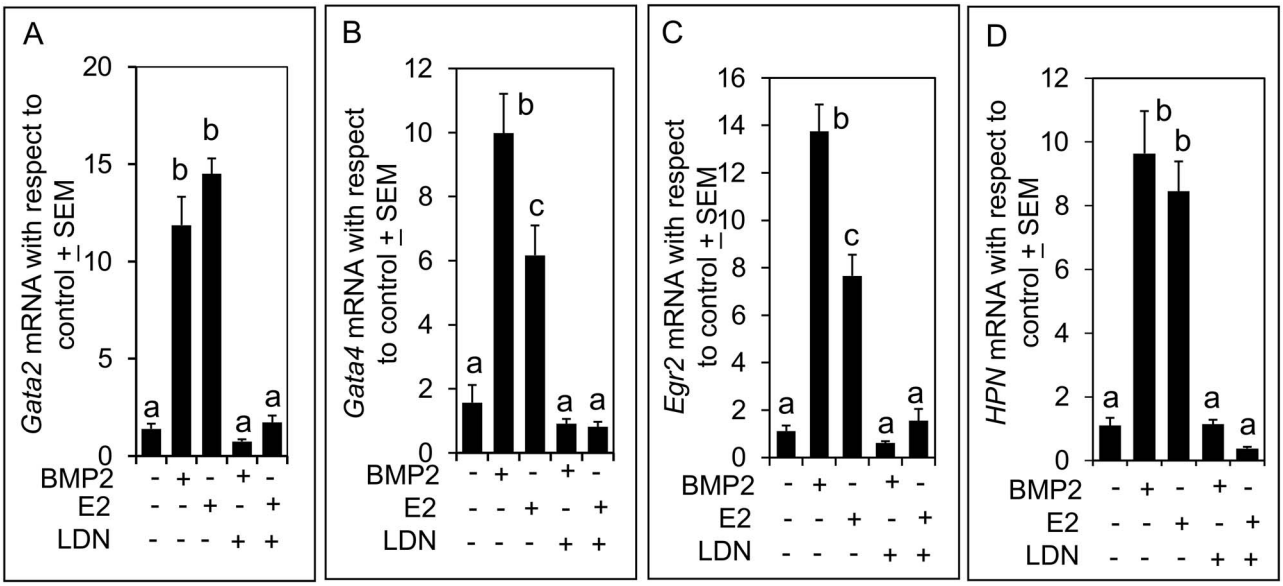

Figure 7. Fold changes in (A) *Gata2*, (B) *Gata4*, (C) *Egr2*, and (D) *HPN* mRNA relative to untreated control in the mouse ovary cultured in vitro for 4 days with or without BMP2, E2, or LDN193,189. ΔCt values for each sample for each transcript were calculated using corresponding *GAPDH* Ct values to obtain ΔΔCt. Then 2^-(ΔΔct) value (fold change relative to untreated control) for each sample was calculated based on the formula provided by the manufacturer (BIO-RAD) and was used to calculate the mean + SEMs. Bars with same letter, $P > 0.05$; bars with different letters, $P < 0.05$.

of *Gata2* depends on the presence of germ cells. Expression of *Gata2*, an immediate BMP effector gene, is essential for the formation of human primordial germ cell-like cell specification [56]. Whether the characteristic increase in GATA2 expression in FOXL2-positive pre-GC in response to BMP2 or E2 reflects a GATA2-mediated transition of SCs into pre-GC warrants further investigation. Granulosa cell-specific localization of GATA4 in the fetal human ovary [57] and adult mouse ovary [58] has been reported and an anti-apoptotic role has been proposed for this TF [57]. Further, E2 appears to upregulate *Gata4* mRNA and protein exclusively in the granulosa cells of young mice [58]. Granulosa cell-specific *Gata4* knockout mice are subfertile with markedly low ovarian estrogen production and compromised FSH-receptor function [59], but no information about PF number is available. The GATA4 has also been shown to play an important role in ovarian morphogenesis in mice [60]. In the present study, increase in *Gata4* mRNA in the ovary and GATA4 immunosignal in FOXL2-positive pre-GC supports the argument that E2 and its potential downstream effector BMP2 may regulate pre-GC and PF formation by upregulating *Gata4* expression. The EGR2 is a member of the early growth response family of zinc finger transcription regulatory factors and the family consists of four members, namely EGR1, EGR2, EGR3, and EGR4 [61, 62]. Each member has specific role in cellular growth, metabolism, and oocyte function [63], but its role in ovarian follicular development remains unclear. Increase in EGR2 expression in pre-GC in response to BMP2 and E2 suggests a possible facilitatory role of EGR2 in SC to pre-GC transition. The EGR2 has been reported to be a survival factor for ovarian granulosa cells, and knockdown of *Egr2* leads to death in KGN cells [64]. Further, LH-induced rapid increase in *Egr2* gene expression in murine granulosa cells [65] suggests that *Egr2* is a target of gonadotropin as well. The exact biological importance of cytoplasmic expression of EGR2 in the oocytes of PF on P1 is not known at present.

Characteristic developmental expression of *HPN* in the mouse ovary during PF formation, and its upregulation by BMP2 or E2 highlight another novel finding in this study. The hepsin is a serine protease of the type II transmembrane serine protease family (TTSP) and has been shown to regulate cell growth [66]. Knockdown of *HPN* expression in ESR1-positive human breast cancer cell line results in a significant decrease in cell proliferation [67]. Loss of tumor suppressor gene, LKB1, in mouse mammary epithelial cells leads to the translocation of hepsin from desmosomes to the cytoplasm coinciding with the degradation of extracellular matrix [68]. Scattered localization of hepsin around FOXL-2-positive pre-GC suggests for its possible association with cell-to-cell integration. Further, remarkable membrane-associated expression of hepsin in BMP2 or E2-exposed ovaries in vitro tends to suggest a possible role of hepsin in epithelial remodeling, especially during oocyte and pre-GC assembly, leading to PF morphology. The hepsin has been shown to activate pro-matrix metalloproteinase 1 (MMP1) and MMP3 in cartilage remodeling [69]. Epithelial fragmentation in the rat ovary at birth when PF formation is in progress coincides with increased expression of MMP1, urokinase-type plasminogen activator, and laminin $\alpha 1$ mRNA [70]. We have reported in the hamster ovary that laminin deposition occurs for the first time when pre-GC and oocyte assemble to form the PF [71]. Therefore, it is tempting to postulate that hepsin may play an important role in BMP2- or E2-regulated remodeling of FOXL2-positive pre-GC and deposition of basement membrane components in order to facilitate oocyte-pre-GC assembly for PF formation. However, we strongly believe that BMP2 or E2 serves as upstream factor, which triggers downstream factors, including various signaling pathways to induce changes in cell functions. Results of the present study support that hypothesis.

Taken together, the results of the present study indicate that BMP2 or E2 modulates a number of key genes, including TFs, which have important role in follicular cell functions and at

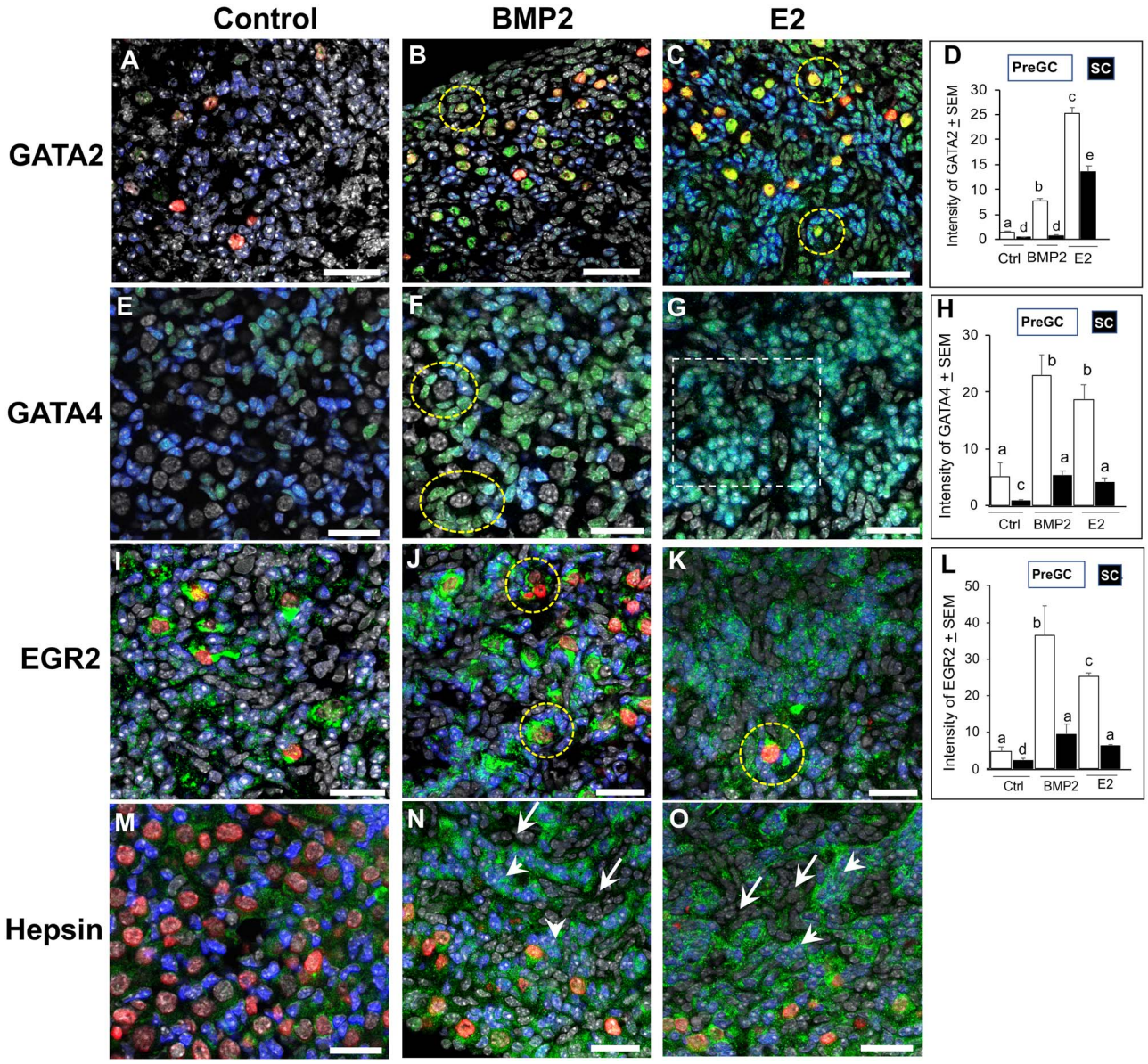

Figure 8. Localization and quantitation of GATA2 (A–D), GATA4 (E–H), EGR2 (I–L), and *Hpn* (M–O) (green) immunosignal in E16 mouse ovaries cultured for 4 days (C0–C4) with vehicle, BMP2, or E2. Broken circles indicate PFs. Magnified views of individual image planes of the area encircled by dotted line is presented in Supplementary Figure 6. Green, GATA2; blue, FOXL2; red, GCNA; gray, nuclei. Bar = 25 μm. In graphs, bars with same letters, $P > 0.05$; bars with different letters, $P < 0.05$.

least one tissue remodeling protease to promote somatic to pre-GC transition and the formation of PFs.

Conflict of interest

The authors have declared that no conflict of interest exists.

Authors' contributions

Conceptualization, methodology, writing—original draft, and writing—review and editing were done by P.C. and S.K.R.; investigation, validation, and formal analysis were done by P.C, R.L.A, and S.K.R; supervision, project administration, and funding acquisition was the responsibility of S.K.R.

Data availability

The sequencing data from RNA-seq have been deposited in GEO under accession number GSE197122.

Acknowledgment

We thank the UNMC genomics core facility for performing RNA sequencing.

References

1. Skinner MK. Regulation of primordial follicle assembly and development. *Hum Reprod Update* 2005; **11**:461–471.
2. De Vos M, Devroey P, Fauser BC. Primary ovarian insufficiency. *Lancet* 2010; **376**:911–921.

3. Pepling ME. Follicular assembly: mechanisms of action. *Reproduction* 2012; **143**:139–149.
4. Bristol-Gould SK, Kreeger PK, Selkirk CG, Kilen SM, Cook RW, Kipp JL, Shea LD, Mayo KE, Woodruff TK. Postnatal regulation of germ cells by activin: the establishment of the initial follicle pool. *Dev Biol* 2006; **298**:132–148.
5. Wang C, Roy SK. Expression of growth differentiation factor 9 in the oocytes is essential for the development of primordial follicles in the hamster ovary. *Endocrinology* 2006; **147**:1725–1734.
6. Yan C, Wang P, DeMayo J, DeMayo FJ, Elvin JA, Carino C, Prasad SV, Skinner SS, Dunbar BS, Dube JL, Celeste AJ, Matzuk MM. Synergistic roles of bone morphogenetic protein 15 and growth differentiation factor 9 in ovarian function. *Mol Endocrinol* 2001; **15**:854–866.
7. Childs AJ, Kinnell HL, Collins CS, Hogg K, Bayne RA, Green SJ, McNeilly AS, Anderson RA. BMP signaling in the human fetal ovary is developmentally regulated and promotes primordial germ cell apoptosis. *Stem Cells* 2010; **28**:1368–1378.
8. Chakraborty P, Roy SK. Bone morphogenetic protein 2 promotes primordial follicle formation in the ovary. *Sci Rep* 2015; **5**:12664.
9. Ying Y, Zhao GQ. Cooperation of endoderm-derived BMP2 and extraembryonic ectoderm-derived BMP4 in primordial germ cell generation in the mouse. *Dev Biol* 2001; **232**:484–492.
10. Shimasaki S, Moore RK, Otsuka F, Erickson GF. The bone morphogenetic protein system in mammalian reproduction. *Endocr Rev* 2004; **25**:72–101.
11. Nakashima K, Yanagisawa M, Arakawa H, Taga T. Astrocyte differentiation mediated by LIF in cooperation with BMP2. *FEBS Lett* 1999; **457**:43–46.
12. Lo L, Sommer L, Anderson DJ. MASH1 maintains competence for BMP2-induced neuronal differentiation in post-migratory neural crest cells. *Curr Biol* 1997; **7**:440–450.
13. Nakamura Y, Ozaki T, Koseki H, Nakagawara A, Sakiyama S. Accumulation of p27 KIP1 is associated with BMP2-induced growth arrest and neuronal differentiation of human neuroblastoma-derived cell lines. *Biochem Biophys Res Commun* 2003; **307**:206–213.
14. Jin H, Pi J, Huang X, Huang F, Shao W, Li S, Chen Y, Cai J. BMP2 promotes migration and invasion of breast cancer cells via cytoskeletal reorganization and adhesion decrease: an AFM investigation. *Appl Microbiol Biotechnol* 2012; **93**:1715–1723.
15. Xiao B, Zhang W, Kuang Z, Lu J, Li W, Deng C, He Y, Lei T, Hao W, Sun Z, Li L. SOX9 promotes nasopharyngeal carcinoma cell proliferation, migration and invasion through BMP2 and mTOR signaling. *Gene* 2019; **715**:144017.
16. Zhao HJ, Chang HM, Zhu H, Klausen C, Li Y, Leung PCK. Bone morphogenetic protein 2 promotes human trophoblast cell invasion by inducing activin A production. *Endocrinology* 2018; **159**:2815–2825.
17. Kashimada K, Pelosi E, Chen H, Schlessinger D, Wilhelm D, Koopman P. FOXL2 and BMP2 act cooperatively to regulate follistatin gene expression during ovarian development. *Endocrinology* 2011; **152**:272–280.
18. Wang C, Roy SK. Development of primordial follicles in the hamster: role of estradiol-17beta. *Endocrinology* 2007; **148**:1707–1716.
19. Wang C, Prossnitz ER, Roy SK. G protein-coupled receptor 30 expression is required for estrogen stimulation of primordial follicle formation in the hamster ovary. *Endocrinology* 2008; **149**:4452–4461.
20. Zachos NC, Billiar RB, Albrecht ED, Pepe GJ. Developmental regulation of baboon fetal ovarian maturation by estrogen. *Biol Reprod* 2002; **67**:1148–1156.
21. Shutt DA, Smith ID, Shearman RP. Oestrone, oestradiol-17beta and oestriol levels in human foetal plasma during gestation and at term. *J Endocrinol* 1974; **60**:333–341.
22. Dutta S, Mark-Kappeler CJ, Hoyer PB, Pepling ME. The steroid hormone environment during primordial follicle formation in perinatal mouse ovaries. *Biol Reprod* 2014; **91**:68–68.
23. Zachos NC, Billiar RB, Albrecht ED, Pepe GJ. Developmental regulation of follicle-stimulating hormone receptor messenger RNA expression in the baboon fetal ovary. *Biol Reprod* 2003; **68**:1911–1917.
24. Greco TL, Payne AH. Ontogeny of expression of the genes for steroidogenic enzymes P450 side-chain cleavage, 3 beta-hydroxysteroid dehydrogenase, P450 17 alpha-hydroxylase/C17-20 lyase, and P450 aromatase in fetal mouse gonads. *Endocrinology* 1994; **135**:262–268.
25. George FW, Wilson JD. Conversion of androgen to estrogen by the human fetal ovary*. *J Clin Endocrinol Metab* 1978; **47**:550–555.
26. Chen Y, Jefferson WN, Newbold RR, Padilla-Banks E, Pepling ME. Estradiol, progesterone, and genistein inhibit oocyte nest breakdown and primordial follicle assembly in the neonatal mouse ovary in vitro and in vivo. *Endocrinology* 2007; **148**:3580–3590.
27. Iguchi T, Takasugi N, Bern HA, Mills KT. Frequent occurrence of polyovular follicles in ovaries of mice exposed neonatally to diethylstibestrol. *Teratology* 1986; **34**:29–35.
28. Zhou S, Turgeman G, Harris SE, Leitman DC, Komm BS, Bodine PVN, Gazit D. Estrogens activate bone morphogenetic protein-2 gene transcription in mouse mesenchymal stem cells. *Mol Endocrinol* 2003; **17**:56–66.
29. Zhou S, Zilberman Y, Wassermann K, Bain SD, Sadovsky Y, Gazit D. Estrogen modulates estrogen receptor alpha and beta expression, osteogenic activity, and apoptosis in mesenchymal stem cells (MSCs) of osteoporotic mice. *J Cell Biochem Suppl* 2001; **Suppl 36**:144–155.
30. Mathieu E, Merregaert J. Characterization of the stromal osteogenic cell line MN7: mRNA steady-state level of selected osteogenic markers depends on cell density and is influenced by 17β-estradiol. *J Bone Miner Res* 1994; **9**:183–192.
31. Chakraborty P, Roy SK. Stimulation of primordial follicle assembly by estradiol-17β requires the action of bone morphogenetic protein-2 (BMP2). *Sci Rep* 2017; **7**:1–10.
32. Roy SK, Wang C, Mukherjee A, Chakraborty P. In vitro culture of fetal ovaries: a model to study factors regulating early follicular development. *Methods Mol Biol* 2012; **825**:151–171.
33. Yu N, Roy SK. Development of primordial and prenatal follicles from undifferentiated somatic cells and oocytes in the hamster prenatal ovary in vitro: effect of insulin. *Biol Reprod* 1999; **61**:1558–1567.
34. Wang X, Pepling ME. Regulation of meiotic prophase one in mammalian oocytes. *Front Cell Dev Biol* 2021; **9**:1–12.
35. Sarma UC, Winship AL, Hutt KJ. Comparison of methods for quantifying primordial follicles in the mouse ovary. *J Ovarian Res* 2020; **13**:1–11.
36. Kim D, Pertea G, Trapnell C, Pimentel H, Kelley R, Salzberg SL. TopHat2: accurate alignment of transcriptomes in the presence of insertions, deletions and gene fusions. *Genome Biol* 2013; **14**:R36.
37. Anders S, Pyl PT, Huber W. HTSeq-A Python framework to work with high-throughput sequencing data. *Bioinformatics* 2015; **31**:166–169.
38. Love MI, Huber W, Anders S. Moderated estimation of fold change and dispersion for RNA-seq data with DESeq2. *Genome Biol* 2014; **15**:550.
39. Yu G, Wang LG, Han Y, He QY. ClusterProfiler: an R package for comparing biological themes among gene clusters. *Omi A J Integr Biol* 2012; **16**:284–287.
40. Subramanian A, Tamayo P, Mootha VK, Mukherjee S, Ebert BL, Gillette MA, Paulovich A, Pomeroy SL, Golub TR, Lander ES, Mesirov JP. Gene set enrichment analysis: a knowledge-based approach for interpreting genome-wide expression profiles. *Proc Natl Acad Sci U S A* 2005; **102**:15545–15550.
41. Sales KU, Hobson JP, Wagenaar-Miller R, Szabo R, Rasmussen AL, Bey A, Shah MF, Molinolo AA, Bugge TH. Expression and genetic loss of function analysis of the HAT/DESC cluster proteases TMPRSS11A and HAT. *PLoS One* 2011; **6**:e23261.
42. Bugge TH, Antalis TM, Wu Q. Type II transmembrane serine proteases. *J Biol Chem* 2009; **284**:23177–23181.

43. Beaufort N, Leduc D, Eguchi H, Mengele K, Hellmann D, Masegi T, Kamimura T, Yasuoka S, Fend F, Chignard M, Pidard D. The human airway trypsin-like protease modulates the urokinase receptor (uPAR, CD87) structure and functions. *Am J Physiol Lung Cell Mol Physiol* 2007; **292**:1263–1272.
44. Yang P, Kriatchko A, Roy SK. Expression of ER-alpha and ER-beta in the hamster ovary: differential regulation by gonadotropins and ovarian steroid hormones. *Endocrinology* 2002; **143**:2385–2398.
45. Viger RS, Guittot SM, Anttonen M, Wilson DB, Heikinheimo M. Role of the GATA family of transcription factors in endocrine development, function, and disease. *Mol Endocrinol* 2008; **22**: 781–798.
46. Padua MB, Fox SC, Jiang T, Morse DA, Tevosian SG. Simultaneous gene deletion of Gata4 and Gata6 leads to early disruption of follicular development and germ cell loss in the murine ovary. *Biol Reprod* 2014; **91**:1–10.
47. Wang JJ, Ge W, Zhai QY, Liu JC, Sun XW, Liu WX, Li L, Lei CZ, Dyce PW, de Felici M, Shen W. Single-cell transcriptome landscape of ovarian cells during primordial follicle assembly in mice. *PLoS Biol* 2020; **18**:1–29.
48. Bayne RA, Donnachie DJ, Kinnell HL, Childs AJ, Anderson RA. BMP signalling in human fetal ovary somatic cells is modulated in a gene-specific fashion by GREM1 and GREM2. *Mol Hum Reprod* 2016; **22**:622–633.
49. Chen Y, Breen K, Pepling ME. Estrogen can signal through multiple pathways to regulate oocyte cyst breakdown and primordial follicle assembly in the neonatal mouse ovary. *J Endocrinol* 2009; **202**:407–417.
50. Dupont S, Krust A, Gansmuller A, Dierich A, Chambon P, Mark M. Effect of single and compound knockouts of estrogen receptors alpha (ERalpha) and beta (ERbeta) on mouse reproductive phenotypes. *Development* 2000; **127**:4277–4291.
51. Emmen JMA, Couse JF, Elmore SA, Yates MM, Kissling GE, Korach KS. In vitro growth and ovulation of follicles from ovaries of estrogen receptor (ER)α and ERβ null mice indicate a role for ERβ in follicular maturation. *Endocrinology* 2005; **146**: 2817–2826.
52. Wang C, Prossnitz ER, Roy SK. Expression of G protein-coupled receptor 30 in the hamster ovary: differential regulation by gonadotropins and steroid hormones. *Endocrinology* 2007; **148**: 4853–4864.
53. Casarini L, Lazzaretti C, Paradiso E, Limoncella S, Riccetti L, Sperduti S, Melli B, Marcozzi S, Anzivino C, Sayers NS, Czapinski J, Brigante G *et al.* Membrane estrogen receptor (GPER) and follicle-stimulating hormone receptor (FSHR) heteromeric complexes promote human ovarian follicle survival. *IScience* 2020; **23**:101812.
54. Niu W, Spradling AC. Two distinct pathways of pregranulosa cell differentiation support follicle formation in the mouse ovary. *Proc Natl Acad Sci U S A* 2020; **117**:20015–20026.
55. Siggers P, Smith L, Greenfield A. Sexually dimorphic expression of Gata-2 during mouse gonad development. *Mech Dev* 2002; **111**: 159–162.
56. Kojima Y, Yamashiro C, Murase Y, Yabuta Y, Okamoto I, Iwatani C, Tsuchiya H, Nakaya M, Tsukiyama T, Nakamura T, Yamamoto T, Saitou M. GATA transcription factors, SOX17 and TFAP2C, drive the human germ-cell specification program. *Life Sci Alliance* 2021; **4**:1–24.
57. Vaskivuo TE, Anttonen M, Herva R, Billig H, Dorland M, te Velde ER, Stenback F, Heikinheimo M, Tapanainen JS. Survival of human ovarian follicles from fetal to adult life: apoptosis, apoptosis-related proteins, and transcription factor GATA-4. *J Clin Endocrinol Metab* 2001; **86**:3421–3429.
58. Heikinheimo M, Ermolaeva M, Bielinska M, Rahman NA, Narita N, Huhtaniemi IT, Tapanainen JS, Wilson DB. Expression and hormonal regulation of transcription factors GATA-4 and GATA-6 in the mouse ovary. *Endocrinology* 1997; **138**:3505–3514.
59. Bennett J, Wu Y-G, Gossen J, Zhou P, Stocco C. Loss of GATA-6 and GATA-4 in granulosa cells blocks folliculogenesis, ovulation, and follicle stimulating hormone receptor expression leading to female infertility. *Endocrinology* 2012; **153**:2474–2485.
60. Efimenko E, Padua MB, Manuylov NL, Fox SC, Morse DA, Tevosian SG. The transcription factor GATA4 is required for follicular development and normal ovarian function. *Dev Biol* 2013; **381**:144–158.
61. O'Donovan KJ, Tourtellotte WG, Milbrandt J, Baraban JM. The EGR family of transcription-regulatory factors: progress at the interface of molecular and systems neuroscience. *Trends Neurosci* 1999; **22**:167–173.
62. Brązert M, Kranc W, Nawrocki MJ, Sujka Kordowska P, Konwerska A, Jankowski M, Kocherova I, Celichowski P, Jeseta M, Ożegowska K, Antosik P, Bukowska D *et al.* New markers for regulation of transcription and macromolecule metabolic process in porcine oocytes during in vitro maturation. *Mol Med Rep* 2020; **21**:1537–1551.
63. Thiel G, Müller I, Rössler OG. Expression, signaling and function of Egr transcription factors in pancreatic β-cells and insulin-responsive tissues. *Mol Cell Endocrinol* 2014; **388**:10–19.
64. Jin H, Won M, Shin E, Kim HM, Lee K, Bae J. EGR2 is a gonadotropin-induced survival factor that controls the expression of IER3 in ovarian granulosa cells. *Biochem Biophys Res Commun* 2017; **482**:877–882.
65. Carletti MZ, Christenson LK. Rapid effects of LH on gene expression in the mural granulosa cells of mouse periovulatory follicles. *Reproduction* 2009; **137**:843–855.
66. Torres-Rosado A, O'Shea KS, Tsuji A, Chou SH, Kurachi K. Hepsin, a putative cell-surface serine protease, is required for mammalian cell growth. *Proc Natl Acad Sci U S A* 1993; **90**: 7181–7185.
67. Xing P, Li JG, Jin F, Zhao TT, Liu Q, Dong HT, Wei XL. Clinical and biological significance of hepsin overexpression in breast cancer. *J Invest Med* 2011; **59**:803–810.
68. Partanen JI, Tervonen TA, Myllynen M, Lind E, Imai M, Katajisto P, Dijkgraaf GJP, Kovanen PE, Mäkelä TP, Wer Z, Klefström J. Tumor suppressor function of Liver kinase B1 (Lkb1) is linked to regulation of epithelial integrity. *Proc Natl Acad Sci U S A* 2012; **109**:E388–397.
69. Wilkinson DJ, Desilets A, Lin H, Charlton S, Del Carmen AM, Falconer A, Bullock C, Hsu YC, Birchall K, Hawkins A, Thompson P, Ferrell WR *et al.* The serine proteinase hepsin is an activator of pro-matrix metalloproteinases: molecular mechanisms and implications for extracellular matrix turnover. *Sci Rep* 2017; **7**:1–13.
70. Mazaud S, Guyot R, Guigon CJ, Coudouel N, Le Magueresse-Battistoni B, Magre S. Basal membrane remodeling during follicle histogenesis in the rat ovary: contribution of proteinases of the MMP and PA families. *Dev Biol* 2005; **277**:403–416.
71. Wang C, Roy SK. Expression of E-cadherin and N-cadherin in perinatal hamster ovary: possible involvement in primordial follicle formation and regulation by follicle-stimulating hormone. *Endocrinology* 2010; **151**:2319–2330.